

## Review

Coupling mechanism of the oxaloacetate decarboxylase Na<sup>+</sup> pump

Peter Dimroth \*, Petra Jockel, Markus Schmid

*Institut für Mikrobiologie, Eidgenössische Technische Hochschule, ETH-Zentrum, Schmelzbergstr. 7, CH-8092 Zürich, Switzerland*

Received 28 June 2000; received in revised form 18 October 2000; accepted 18 October 2000

---

**Abstract**

The oxaloacetate decarboxylase Na<sup>+</sup> pump consists of subunits  $\alpha$ ,  $\beta$  and  $\gamma$ , and contains biotin as the prosthetic group. The peripheral  $\alpha$  subunit catalyzes the carboxyltransfer from oxaloacetate to the prosthetic biotin group to yield the carboxybiotin enzyme. Subsequently, this is decarboxylated in a Na<sup>+</sup>-dependent reaction by the membrane-bound  $\beta$  subunit. The decarboxylation is coupled to Na<sup>+</sup> translocation from the cytoplasm into the periplasm, and consumes a periplasmically derived proton. The  $\gamma$  subunit contains a Zn<sup>2+</sup> metal ion which may be involved in the carboxyltransfer reaction. It is proposed to insert with its N-terminal  $\alpha$ -helix into the membrane and to form a complex with the  $\alpha$  subunit with its water-soluble C-terminal domain. The  $\beta$  subunit consists of nine transmembrane  $\alpha$ -helices, a segment (IIIa) which inserts from the periplasm into the membrane but does not penetrate it, and connecting hydrophilic loops. The most highly conserved regions of the molecule are segment IIIa and transmembrane helix VIII. Functionally important residues are D203 (segment IIIa), Y229 (helix IV) and N373, G377, S382 and R389 (helix VIII). The polar of these amino acids may constitute a network of ionizable groups which promotes the translocation of Na<sup>+</sup> and the oppositely oriented translocation of H<sup>+</sup> across the membrane. Evidence indicates that two Na<sup>+</sup> ions are bound simultaneously to subunit  $\beta$  with D203 and S382 acting as binding sites. Sodium ion binding from the cytoplasm to both sites elicits decarboxylation of carboxybiotin possibly with the consumption of the proton extracted from S382 and delivered via Y229 to the carboxylated prosthetic group. A conformational change exposes the bound Na<sup>+</sup> ions toward the periplasm. With H<sup>+</sup> entering from the periplasm, the hydroxyl group of S382 is regenerated, and as a consequence, the Na<sup>+</sup> ions are released into this compartment. After switching back to the original conformation, Na<sup>+</sup> pumping continues. © 2001 Elsevier Science B.V. All rights reserved.

**Keywords:** Oxaloacetate decarboxylase; Na<sup>+</sup> pump mechanism, direct coupling; Active site residue

---

**1. Introduction**

Protons are the predominant coupling ions in energy conversions by bacterial membranes. A number of distinct systems have been recognized, however, which use Na<sup>+</sup> as the coupling ion (for recent re-

views see [1,2]). An overview of bioenergetic processes coupled to Na<sup>+</sup> circulation is shown in Fig. 1. On one hand, a number of primary Na<sup>+</sup> extruding pumps have been recognized and on the other hand, the Na<sup>+</sup> gradient thus established is used to perform work. The Na<sup>+</sup> extruding pumps are certain biotin-containing decarboxylases [3–6], the respiratory NADH:ubiquinone oxidoreductases of *Vibrio alginolyticus* [7,8], *Klebsiella pneumoniae* [9], or *Escherichia coli* [10], the Na<sup>+</sup> translocating methyltetrahydromethanopterin:coenzyme M methyltransferase

---

\* Corresponding author. Fax: +41-1-6321378;  
E-mail: dimroth@micro.biol.ethz.ch

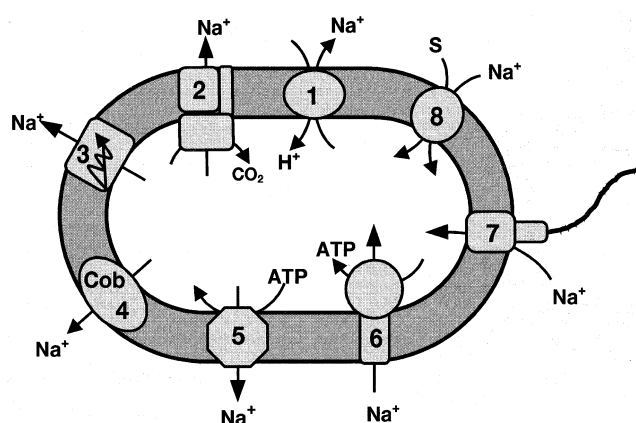


Fig. 1. Schematic overview of bioenergetic processes coupled to  $\text{Na}^+$  circulation. The electrochemical sodium ion gradient is generated either by a proton-driven  $\text{Na}^+/\text{H}^+$  antiporter (1), by a decarboxylase (2), respiratory enzymes (3),  $N^5$ -methyltetrahydromethanopterin:coenzyme M methyltransferase (4), or a V-type ATPase (5). The established sodium motive force then provides the energy for ATP synthesis by an  $\text{F}_1\text{F}_0$  ATP synthase (6), for movement of flagellar motors (7), or for solute uptake (8). Please note that the systems depicted here are from different bacteria.

of methanogens with the cofactor cobalamin [11,12] or ATPases of the V-type [13]. Alternatively, the  $\text{Na}^+$  gradient can be established by secondary  $\text{Na}^+/\text{H}^+$  antiporters [14] with the electrochemical  $\text{H}^+$  gradient as the driving force. The  $\text{Na}^+$  gradient can be used to drive solute uptake ([15] and references therein), flagellar motion [16] or the synthesis of ATP by an F-type ATP synthase [17]. A prominent example of an ATP synthesis mechanism by  $\text{Na}^+$  cycling is *Propionigenium modestum*. This anaerobic bacterium generates an electrochemical  $\text{Na}^+$  gradient ( $\Delta\mu\text{Na}^+$ ) with the methylmalonyl-CoA decarboxylase  $\text{Na}^+$  pump and utilizes the  $\Delta\mu\text{Na}^+$  thus established to drive ATP synthesis by the  $\text{F}_1\text{F}_0$  ATP synthase [18,19].

The  $\text{Na}^+$  transport decarboxylases represent a family of enzymes that use the free energy of decar-

boxylation reactions to pump  $\text{Na}^+$  ions out of the cell into the environment. Table 1 compiles several members of this family. In the case of oxaloacetate decarboxylase, methylmalonyl-CoA decarboxylase and glutaconyl-CoA decarboxylase, each substrate is sufficiently activated for the decarboxylation reaction: as a  $\beta$ -ketoacid, oxaloacetate decarboxylates readily; methylmalonyl-CoA or glutaconyl-CoA are activated for decarboxylation by the  $\beta$ -thioester group or by its vinyllogue, respectively.

Interestingly, in *Malonomonas rubra*, a  $\text{Na}^+$  pumping decarboxylase was identified which converts malonate into acetate and  $\text{CO}_2$  [6]. As malonate at physiological pH exists mainly as the dianion which is rather inert chemically, the malonate decarboxylase is more complicated and involves an activation module that converts the free malonate into a malonyl-thioester with the 2'-(5"-phosphoribosyl)-3'-dephospho coenzyme A prosthetic group of the enzyme [24,25]. Only in this form is the malonate sufficiently activated to become decarboxylated. The mechanism of the decarboxylation of the malonyl-S enzyme itself is very similar to the decarboxylation mechanism of the other  $\text{Na}^+$  transport decarboxylases.

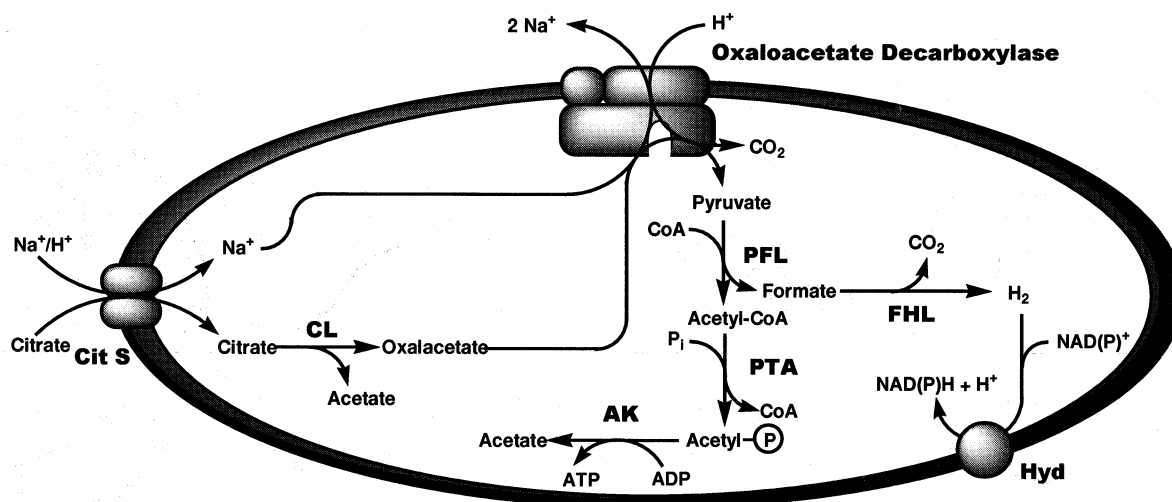
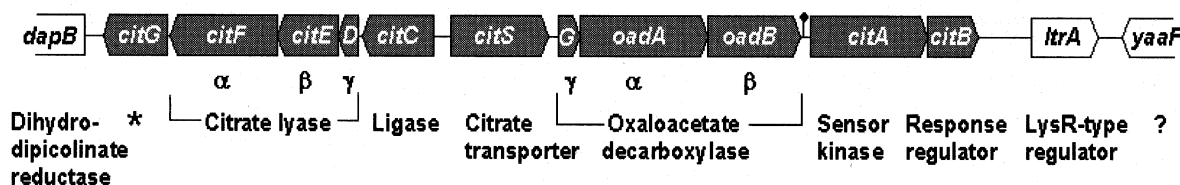
## 2. Physiology of oxaloacetate decarboxylase

Oxaloacetate decarboxylase was the first enzyme of the  $\text{Na}^+$  transport decarboxylase family demonstrated to act as a primary  $\text{Na}^+$  pump [3]. The enzyme performs a prominent role in anaerobic citrate metabolism as shown in Fig. 2A [1,2]. After citrate uptake by a  $\text{Na}^+$ -dependent citrate carrier [15], the tricarboxylic acid is split into oxaloacetate and acetate by citrate lyase. Oxaloacetate is subsequently decarboxylated to pyruvate by the membrane-bound oxaloacetate decarboxylase, and the free energy of

Table 1  
Members of the family of  $\text{Na}^+$  transport decarboxylases

Decarboxylase	Bacterium	Subunit composition <sup>a</sup>	References
Oxaloacetate decarboxylase	<i>K. pneumoniae</i>	<u><math>\alpha</math></u> (63.4), $\beta$ (44.9), $\gamma$ (8.9)	[20,21]
Methylmalonyl-CoA decarboxylase	<i>Veillonella parvula</i>	$\alpha$ (55.0), $\beta$ (38.7), <u><math>\gamma</math></u> (12.9), $\delta$ (11.9), $\epsilon$ (5.8)	[22]
Glutaconyl-CoA decarboxylase	<i>Acidaminococcus fermentans</i>	$\alpha$ (64.3), $\beta$ (36), <u><math>\gamma</math></u> (24), $\delta$ (14)	[23]
Malonate decarboxylase	<i>Malonomonas rubra</i>	MadB (43), MadC (34.9), MadD (31.8), <u>MadF</u> (7.4)	[24]

<sup>a</sup>The molecular mass is indicated in parentheses (kDa). The biotin-containing subunit is underlined.

**A****B**

\* involved in the biosynthesis of enzymatically active citrate lyase

Fig. 2. (A) Schematics of the citrate fermentation pathway in *K. pneumoniae* and location of the enzymes involved. Citrate is transported into the cell by the  $\text{Na}^+$ -specific transporter CitS. Internal citrate is cleaved by citrate lyase (CL) to acetate and oxaloacetate. The latter is decarboxylated to pyruvate by the oxaloacetate decarboxylase  $\text{Na}^+$  pump. Pyruvate formate lyase (PFL) forms formate and acetyl-CoA from pyruvate. Acetyl-CoA is converted to acetyl-phosphate by phosphotransacetylase (PTA) and further to acetate with ATP generation by the acetate kinase (AK) reaction. Formate is split into  $\text{CO}_2$  and  $\text{H}_2$  by formate hydrogen lyase (FHL) and the  $\text{H}_2$  is utilized for NAD(P) reduction by a membrane-bound hydrogenase (Hyd). (B) Physical map of the DNA segment from *K. pneumoniae* with the genes for the citrate fermentation enzymes forming a regulon. The function of the gene products is indicated.

the decarboxylation reaction is utilized for  $\text{Na}^+$  ion pumping out of the cell. Pyruvate is further degraded to acetyl-CoA and formate and from the former acetyl-phosphate is produced. This reacts with ADP to acetate and ATP. Also of interest in this pathway is the synthesis of NADH for biosynthetic reactions. Unlike most other anaerobic bacteria which are faced with the problem of keeping the redox balance by NADH oxidizing reactions, *K. pneumoniae* growing on the highly oxidized substrate citrate must generate NADH for biosynthetic reactions. The citric acid cycle is not feasible for this purpose because

$\alpha$ -ketoglutarate dehydrogenase synthesis is repressed anaerobically. The NADH biosynthetic pathway rather involves the generation of  $\text{H}_2$  by the formate hydrogen lyase and reduction of  $\text{NAD}^+$  with  $\text{H}_2$  by a membrane-bound hydrogenase [26].

Overall, the citrate fermentation pathway produces 1 mol ATP per mol citrate, and in addition, an electrochemical gradient of  $\text{Na}^+$  ions is generated. The latter is used in part to drive citrate uptake into the cell by the electroneutral  $\text{Hcitrate}^{2-}/\text{Na}^+/\text{H}^+$  symporter [15]. The electrical component of the  $\Delta\mu\text{Na}^+$  generated by the oxaloacetate decarboxylase  $\text{Na}^+$

pump is likely to contribute driving force to the synthesis of ATP by the  $H^+$  translocating  $F_1F_0$  ATP synthase, which is constitutively synthesized by *K. pneumoniae*.

The genes that are specifically required for citrate fermentation are clustered on the *K. pneumoniae* chromosome [27,28]. The physical map of this region, shown in Fig. 2B, indicates the *citS* gene encoding the  $Na^+$ -dependent citrate carrier succeeded by the three genes for the oxaloacetate decarboxylase (*oadGAB*) and the two-component regulatory system *citA/B*. The cluster is completed by the divergently oriented *citCDEFG* genes encoding citrate lyase ligase (*citC*), the three subunits of citrate lyase (*citDEF*), and an enzyme involved in the biosynthesis of the 2'-(5"-phosphoribosyl)-3'-dephospho-CoA prosthetic group of citrate lyase (*citG*) [29].

### 3. Subunits of the oxaloacetate decarboxylase $Na^+$ pump

Fig. 3 shows a cartoon of the structure and function of the oxaloacetate decarboxylase  $Na^+$  pump. The enzyme is composed of three different subunits  $\alpha$ ,  $\beta$ , and  $\gamma$  in a 1:1:1 stoichiometry [30,31]. The peripheral membrane-bound subunit  $\alpha$  (63.5 kDa) has two different domains, an N-terminal carboxyltransferase domain and a C-terminal biotin binding

domain [20]. These two domains are connected by an extended proline/alanine linker peptide. The biotin binding domain has a covalently linked biotin prosthetic group at a lysine residue located 35 residues before the C-terminus. The  $\beta$  subunit (44.9 kDa) is highly hydrophobic and therefore intimately associated with the membrane [21]. The  $\gamma$  subunit (8.9 kDa) consists of an N-terminal membrane anchor, followed by a proline/alanine linker and a hydrophilic C-terminal domain including a polyhistidine motif which is believed to contribute ligands for the binding of a  $Zn^{2+}$  metal ion [32,33]. Probably by interacting with its water-soluble portion with the  $\alpha$  subunit and with its integral membrane-bound portion with the  $\beta$  subunit, the  $\gamma$  subunit is fundamental for the stability of the oxaloacetate decarboxylase multisubunit complex [33].

The catalytic cycle performed by this machinery starts with the binding of oxaloacetate to the carboxyltransferase site on the  $\alpha$  subunit [30]. Subsequently, the carboxyl group from position 4 of oxaloacetate is transmitted to the biotin prosthetic group. Facilitated by the flexible proline/alanine linker, the carboxybiotin switches from the carboxyltransferase site on the  $\alpha$  subunit to the decarboxylase site on the  $\beta$  subunit. Here, decarboxylation of carboxybiotin takes place with the consumption of a periplasmically derived proton [34]. Simultaneously, two  $Na^+$  ions are pumped into the periplasmic compartment across the membrane [35]. Intimately associated with the chemical reactions occurring in this cycle are conformational changes of the protein, e.g. the flipping of the prosthetic group between the two catalytic sites or the opening and closing of  $Na^+$  access channels toward the cytoplasmic or periplasmic surface of the membrane (see below).

The oxaloacetate decarboxylase enzyme complex can be conveniently isolated in amounts of 10–20 mg per prep by solubilizing the enzyme from the membrane with detergent and subsequent affinity chromatography on a monomeric avidin-Sepharose column [36]. The three-subunit complex of *K. pneumoniae* has also been synthesized in *E. coli* in a catalytically competent form [33] which offers the possibility of studying the enzyme with the mutational approach. Furthermore, we were able to isolate the two-subunit complexes  $\alpha\gamma$  and  $\beta\gamma$ , respectively, as well as the  $\alpha$  subunit in high amounts [33].

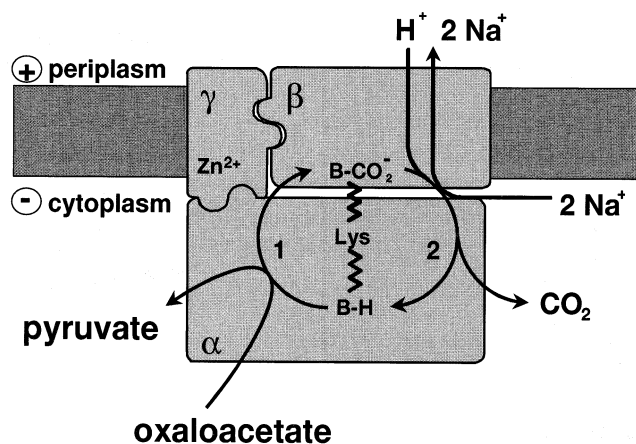


Fig. 3. Cartoon showing the overall geometry of the oxaloacetate decarboxylase and features of the catalytic events. B-H, biotin;  $B-CO_2^-$ , carboxybiotin; Lys, biotin binding lysine residue; (1) carboxyltransferase reaction and (2) decarboxylase reaction.

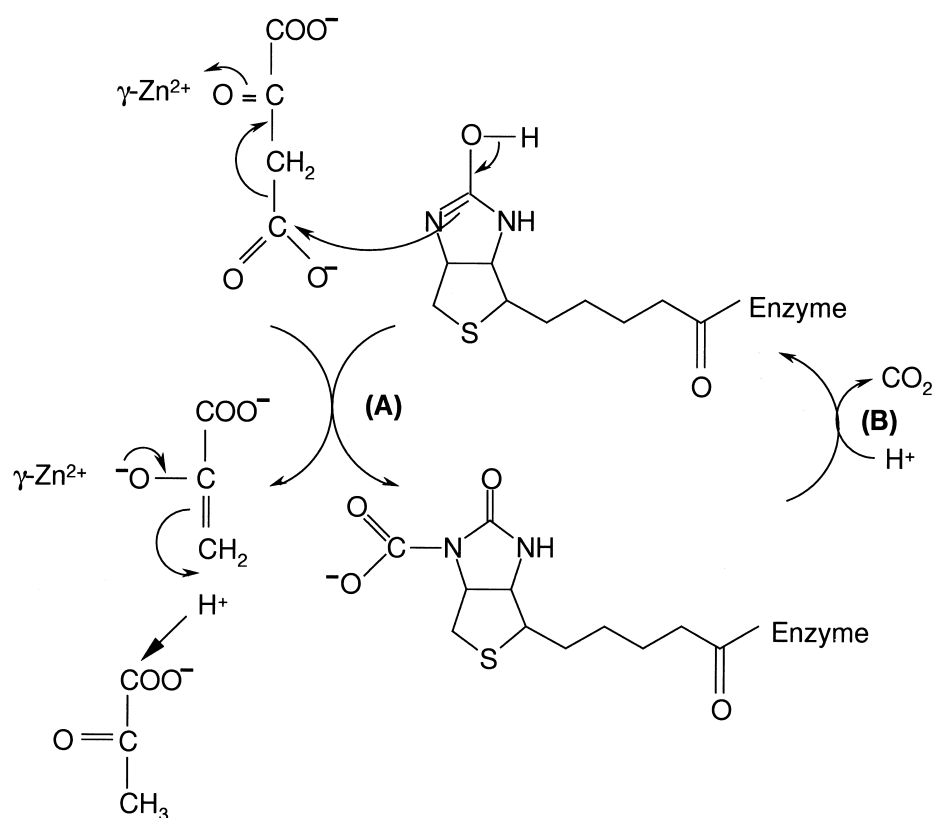


Fig. 4. Hypothetical reaction mechanism of the carboxyltransfer reaction with the  $\text{Zn}^{2+}$  metal ion facilitating C-C bond cleavage in oxaloacetate (A). Also shown is the consumption of a proton in the carboxybiotin decarboxylation reaction (B).

#### 4. Role of the $\text{Zn}^{2+}$ metal ion in catalysis of the carboxyltransfer reaction

The decarboxylase contains 1 mol tightly bound  $\text{Zn}^{2+}$  per mol enzyme which is attached to the  $\gamma$  subunit. Three histidine residues near the C-terminus of this protein are candidate ligands for the binding of  $\text{Zn}^{2+}$  and indeed  $\text{Zn}^{2+}$  binding is abolished upon consecutively deleting these histidine residues (unpublished results). We propose that the  $\text{Zn}^{2+}$  ion plays an important role in the catalysis of the carboxyltransfer reaction. As shown in Fig. 4, the  $\text{Zn}^{2+}$  ion coordinating to the carbonyl oxygen atom of oxaloacetate withdraws electrons from this atom, thereby facilitating the C-C bond cleavage of oxaloacetate to generate pyruvate and the carboxybiotin enzyme derivative. With the  $\alpha$  subunit alone, the carboxyltransfer reaction can be monitored by forming the  $^{14}\text{C}$ carboxybiotin protein upon incubation with  $[4\text{-}^{14}\text{C}]$ oxaloacetate. Interestingly, the rate of the carboxyltransferase reaction was two to three

orders of magnitude too low to account for the physiological turnover of this enzyme and increased considerably to values that could not be resolved within the time resolution of our measurements by adding the  $\gamma$  subunit [33]. These results are in agreement with the notion that the  $\gamma$  subunit with its  $\text{Zn}^{2+}$  metal ion participates directly in the catalytic mechanism of the carboxyltransferase.

#### 5. Membrane topology of the $\beta$ subunit

The  $\beta$  subunit is a very hydrophobic protein consisting of 433 amino acid residues. According to hydropathy analysis the protein may span the membrane nine or 10 times. Several different approaches have been taken to determine the membrane topology of the  $\beta$  subunit. These included analyses of various truncated forms of the molecule fused to alkaline phosphatase or  $\beta$ -galactosidase and accessibility of engineered cysteine residues from the two

different sides of the membrane. From the combined results of these analyses, the topological model shown in Fig. 5 has been derived [37]. Fusion sites yielding positive alkaline phosphatase activity, which are indicative of a periplasmic location, are shown in yellow. Those with no or very low alkaline phosphatase activity indicate a cytoplasmic location and are shown in white. Positive  $\beta$ -galactosidase fusions are shown in green and indicate a cytoplasmic location of the fusion site. Those fusions without  $\beta$ -galactosidase activity which indicate a periplasmic location of the fusion site are shown in red. Cysteine residues which become labeled from the periplasmic side are shown in blue squares and those which become labeled from the cytoplasmic side are shown in green squares. Those cysteines which are not accessible for alkylation from either side of the membrane are shown in white squares. The model derived from all these results has the N-terminus in the cytoplasm and the C-terminus in the periplasm. It has been proposed that the protein folds into a block of three

N-terminal helices with a large cytoplasmic loop connecting helices II and III. This folding is in accord with most of the fusion results and with the sidedness of engineered cysteine residues. Exceptions are the two positive *phoA* and *lacZ* fusions in the N-terminal portion of the large cytoplasmic loop linking helices II and III. For loops of this size, however, the topological analysis with the fusion technique is known to give unpredictable results. The topology analyses further indicated the folding into a block of six helices forming the C-terminal portion of the molecule. The domain between the N-terminal and the C-terminal block has been termed region IIIa and appears to fold in an unusual manner. The peptide from residues 179 to 189 appears to form a loop; it is not conserved and has deletions in some of the related molecules of the family. The data on the topology of this peptide further indicate a periplasmic location. This location rules out the folding of region IIIa into two additional helices that fully span the membrane. Instead, an insertion from the periplasmic surface

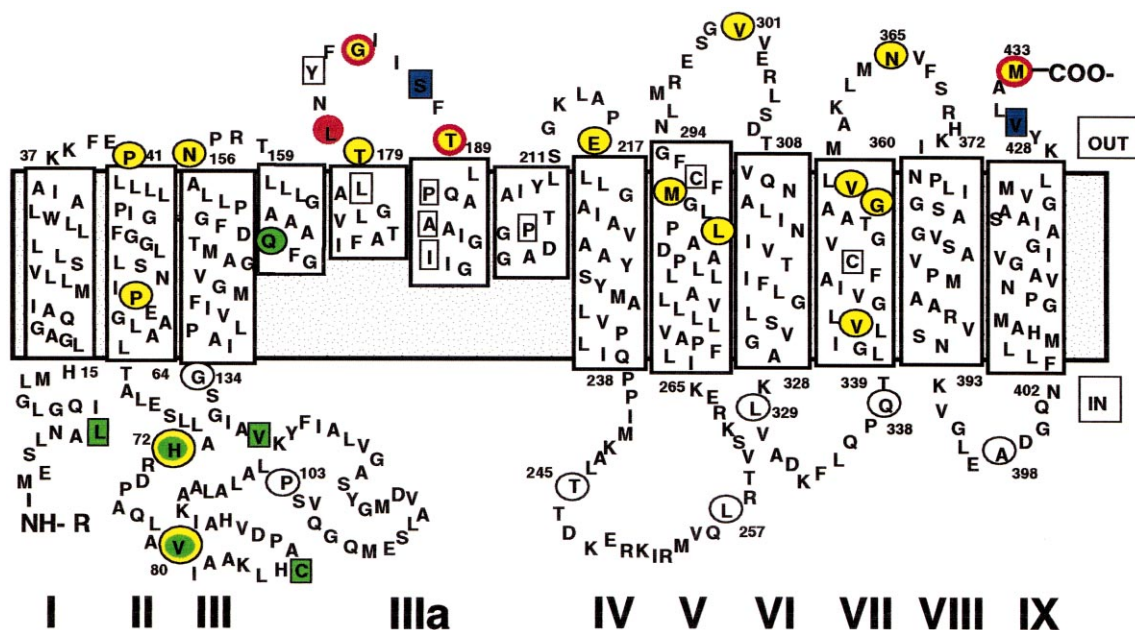


Fig. 5. Topological model of the oxaloacetate decarboxylase  $\beta$  subunit. The amino acid residues to which the signal sequence-depleted alkaline phosphatase (PhoA) or  $\beta$ -galactosidase (LacZ) was fused are marked by circles. Fusion sites yielding clones with positive alkaline phosphatase activities ( $>5$  units, blue colonies) are yellow, and those with negative alkaline phosphatase activities ( $<5$  units, white colonies) are white. Fusion sites yielding clones with positive  $\beta$ -galactosidase activities ( $>350$  units) are green, and those with negative  $\beta$ -galactosidase activities ( $<50$  units) are red. The yellow circles outlined in red mean red and yellow circles, i.e. negative LacZ and positive PhoA fusions. The green circles outlined in yellow mean green and yellow circles, i.e. positive LacZ and positive PhoA fusions. The amino acid residues which had been changed to cysteines are indicated by squares. Cysteines which are labeled from the cytoplasmic side are green, those which are labeled from the periplasmic side blue, and those which are not labeled from either side white.

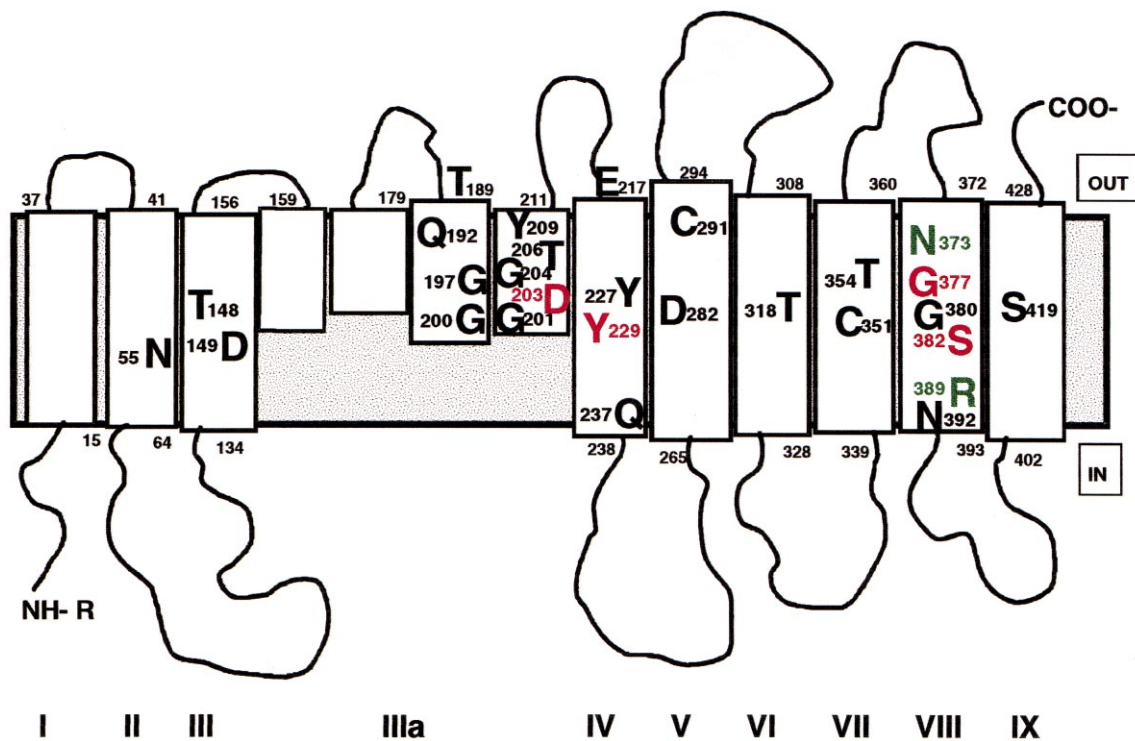


Fig. 6. Location of the amino acids within the  $\beta$  subunit of oxaloacetate decarboxylase which have been changed by site-specific mutagenesis. Residues marked in red led to an inactive mutant enzyme, residues marked in green led to mutant specimens with severely reduced activities, and residues marked in black led to mutant specimens which were not significantly affected in their catalytic capabilities.

into the membrane is suggested, but without penetrating it all the way to the cytoplasmic surface. The C-terminal portion of region IIIa is of special interest not only due to its unusual folding within the membrane but also because it contains the invariable D203 residue. This amino acid is located within the most highly conserved area of the molecule comprising seven invariant consecutive residues. It will be shown below that D203 cannot be replaced by any amino acid without the complete loss of oxaloacetate decarboxylase activity [34].

## 6. Site-specific mutagenesis of the $\beta$ subunit

In order to identify the functionally important residues of the  $\beta$  subunit, a site-specific mutagenesis approach was performed. A particular advantage of this investigation was the availability of the sequences of several related proteins, because this made it possible to select specific amino acids for mutation. We reasoned that only those residues could be func-

tionally important that are conserved in all proteins or have undergone conservative exchanges. Furthermore, we considered polar residues within membrane-spanning domains the most interesting ones to mutate because these were the key candidates for participating in  $\text{Na}^+$  or  $\text{H}^+$  transport across the membrane. Fig. 6 summarizes all amino acids of OadB that have been mutated [34,35,39]. Residues shown in red yielded an inactive oxaloacetate decarboxylase activity after mutagenesis, mutations in green indicate residues severely reduced in decarboxylase activity and mutations in black indicate residues not significantly affected in activity of the enzyme. Of particular interest are the catalytically inactive mutants of D203 (region IIIa) [34], of Y229 (helix IV) [39], and of G377 or S382 (helix VIII) [35]. The first functionally indispensable residue identified was D203 in region IIIa. No other residue was tolerated at this position and even the most conservative exchanges of D203 to E, N, or Q led to the complete loss of oxaloacetate decarboxylase activity. As expected, the mutated enzymes were also inactive



as  $\text{Na}^+$  pumps. This was demonstrated with an in vivo assay using the *E. coli* strain EP432 which has deletions in both  $\text{Na}^+/\text{H}^+$  antiporters [38]. Due to this deficiency, this strain is unable to grow at pH 6 on a glucose mineral medium in the presence of 350 mM NaCl. After transformation with a plasmid harboring the genes for the oxaloacetate decarboxylase, the antiporter deletion strain regains the capacity to grow at elevated  $\text{Na}^+$  concentrations, apparently because toxic intracellular  $\text{Na}^+$  concentrations are diminished by the activity of the oxaloacetate decarboxylase  $\text{Na}^+$  pump [35]. However, if as in the case of the D203 mutant enzymes lacking the  $\text{Na}^+$  pumping activity were synthesized in *E. coli* EP432, the defect could not be complemented and growth at elevated  $\text{Na}^+$  concentrations was not observed.

The carboxyltransferase activity, which is catalyzed by OadA [31], was not affected by the  $\beta$  D203 mutations, as expected [34]. The enzyme catalyzed rapid  $^{14}\text{CO}_2$  transfer from  $[4\text{-}^{14}\text{C}]$ oxaloacetate to its prosthetic biotin group. The  $[^{14}\text{C}]$ carboxybiotin enzyme derivative thus derived was stable even in the presence of  $\text{Na}^+$  ions, indicating the complete knock-out of the carboxybiotin decarboxylase activity. In the wild-type enzyme, however, the carboxybiotin enzyme is immediately decarboxylated and cannot be isolated as a stable intermediate. From these results we conclude that D203 is specifically required for the decarboxylation of carboxybiotin and the transport of  $\text{Na}^+$  that is coupled to it. Hence, D203 may serve a dual role as  $\text{Na}^+$  binding site for the transport of this alkali ion and as proton carrier for guiding protons in the opposite direction across the membrane into the catalytic site for the decarboxylation of carboxybiotin (see below).

The functioning of the carboxybiotin decarboxylase  $\text{Na}^+$  pump also depends heavily on S382 of helix VIII. If this residue is exchanged to A, C, E, N, or Q, oxaloacetate decarboxylase and  $\text{Na}^+$  transport activities are completely abolished while the carboxyltransferase activity is retained [35]. In mutants with the conservative S382T exchange, oxaloacetate decarboxylase and  $\text{Na}^+$  transport activities were retained. More importantly, these activities were also partially retained in the S382D mutant.

The properties of these mutations are insightful for the function of S382 in the transport of  $\text{Na}^+$  and in the decarboxylation of carboxybiotin. All residues

tolerated at position 382 carry a hydroxyl group or an acidic side chain (S, T, or D) that may deliver its proton into the catalytic site, thus initiating the  $\text{H}^+$ -consuming decarboxylation of carboxybiotin. An exclusive role of S382 as proton carrier is unlikely, however, because S382C and S382E mutations are inactive, whereas S382D is active. Hence, the length of the side chain of the residue at position 382 is as crucial for the activity as the presence of a group that may give up a proton. If the residue at position 382 also functions as a  $\text{Na}^+$  binding site, extending the side chain from D to E may disturb the coordination sphere for the alkali ion so that  $\text{Na}^+$  is no longer able to bind. For these reasons, we propose a dual function for S382, serving as a  $\text{Na}^+$  binding site during the transport of this alkali ion into the periplasm and as a  $\text{H}^+$  binding site for guiding protons in the opposite direction through the membrane into the catalytic site. Hence, S382 could perform a role similar to that of D203, and both residues could be part of a  $\text{Na}^+$  and  $\text{H}^+$  translocation network within the membrane. To function in proton conduction, the side chain hydroxyl of S382 has to switch between the protonated and deprotonated states. In aqueous environments, the hydroxyl group of serine has a  $\text{pK} > 13$  and therefore does not deprotonate under physiological conditions. However, as exemplified for the serine proteases, abstraction of the proton from serine is feasible with a histidine aspartate pair acting as a base within a hydrophobic pocket of the enzyme. A candidate to take over a proton from S382 in OadB is the R389–carboxybiotin pair. The R389 residue is located two helical turns away from S382 toward the cytoplasm, and both residues have their side chains exposed to the same side. Furthermore, R389 is conserved among species, except for the conservative R389K exchange in the malonate decarboxylase  $\beta$  subunit. Mutational analyses support the proposal of an intimate interaction between S382 and R389 in the proton-conducting pathway. While the R389K mutant exhibited almost wild-type oxaloacetate decarboxylase activity and was a functional  $\text{Na}^+$  pump, all the other mutants that were investigated had severely reduced decarboxylase and impaired  $\text{Na}^+$  pumping activities as judged from growth assays with the  $\text{Na}^+$ -sensitive *E. coli* EP432 strain (see above). An increase in the pH optimum of the decarboxylase by about two units in the R389A



or R389L mutants compared to that of the wild-type is further in accord with the proposed proton conduction from S382 via R389 to carboxybiotin, where it initiates the decarboxylation of this acid-labile compound [35].

Other amino acids of interest in helix VIII are G377 and N373. Glycine at position 377 was absolutely essential and not even an exchange by alanine was tolerated. Hence, this glycine residue could be at a sterically sensitive position within the molecule which could involve either the  $\text{Na}^+$  conducting channel itself or a contact site with another helix. In the N373L or N373D mutants the oxaloacetate decarboxylase activity dropped to about 1–2% of that of the wild-type, indicating that N373 is required for an efficient functioning of the enzyme but does not have an irreplaceable role for the catalysis.

Another interesting region of the  $\beta$  subunit are two conserved tyrosine residues in helix IV (Y227 and Y229). If tyrosine 227 is mutated to alanine, the specific oxaloacetate decarboxylase activity dropped from 45 U/mg (wild-type) to 0.5 U/mg protein, but Y227C and Y227F mutated enzymes are more active yielding 12 and 9 U/mg, respectively [39]. From these data, it is clear that Y227 is an important residue to ensure a high catalytic activity of the enzyme but it is not indispensable for function. Tyrosine 229, however, appears to be fundamentally important for function. The conservative exchange of this tyrosine residue by phenylalanine completely abolished the oxaloacetate decarboxylase and  $\text{Na}^+$  transport activities. As with the other inactive mutants described, this effect results from the destruction of the carboxybiotin decarboxylase: upon incubation with [4- $^{14}\text{C}$ ]-oxaloacetate, a stable [ $^{14}\text{C}$ ]carboxybiotin enzyme derivative was formed, indicating that the carboxyl-transferase activity was intact and the decarboxylase activity was abolished. Tyrosine 229 has also been exchanged to alanine. Interestingly, this non-conservative mutant retained marginal but measurable oxaloacetate decarboxylase activity. This activity was too low to observe  $\text{Na}^+$  pumping in the *in vivo* system (see above) but a stable [ $^{14}\text{C}$ ]carboxybiotin enzyme was not formed due to the residual carboxybiotin decarboxylase activity. In a model, presented below, Y229 is proposed to participate in the proton conduction network that leads to the decarboxylation of carboxybiotin. Accordingly, phenylalanine,

which has nearly the same dimensions as tyrosine but lacks the phenolic hydroxyl, is an unsuitable substitute. An alanine residue, on the other hand, might leave enough space for a water molecule to contact S382 instead of Y229. This water may take over the role of Y229 in the proton conduction network, albeit at a much slower rate.

## 7. Additional information gained with perspectives to the mechanism

The oxaloacetate decarboxylase  $\text{Na}^+$  pump has been intensively studied biochemically and some of these results that are of relevance for the catalytic mechanism will be presented below. One of the questions was whether  $\text{H}_2\text{O}$  or a proton was the substrate for the decarboxylation of the carboxybiotin enzyme. In the first case, bicarbonate would be released as product, whereas  $\text{CO}_2$  would be the product with  $\text{H}^+$  as the substrate. Oxaloacetate decarboxylation was accompanied by a significant alkalization of the environment [30]. Subsequently, the pH decreased again to levels only slightly higher than before decarboxylation was initiated. In the presence of carboanhydrase, which accelerates the equilibration between  $\text{CO}_2$  and  $\text{H}_2\text{CO}_3$ , the alkaline overshoot was not observed and the pH increased continuously to its final level. These results clearly indicate that protons are consumed and  $\text{CO}_2$  is released as the product. In the absence of carboanhydrase,  $\text{CO}_2$  hydrates only slowly and the new equilibrium pH is therefore only reached after the observed large alkaline overshoot.

The next important question was from which side of the membrane the proton derives that is consumed in the decarboxylation of carboxybiotin. A hint to answer this question came from studying the effect of ionophores on the  $\text{Na}^+$  pumping activity of oxaloacetate decarboxylase reconstituted into proteoliposomes. It was observed that the rate of  $\text{Na}^+$  transport increased in the presence of valinomycin ( $+\text{K}^+$ ) as expected for an electrogenic pump [34]. Surprisingly, however, the  $\text{Na}^+$  transport rate was hardly effected by the electrogenic protonophore CCCP. These data could be explained if the protons consumed in the decarboxylation reaction derive from the interior compartment of the proteoliposomes

which consequently gets alkaline. Valinomycin-induced  $K^+$  movements will thus dissipate the rate-limiting membrane potential easily, but CCCP-induced  $H^+$  movements would have to proceed against the  $\Delta pH$  and are therefore unfavorable. Alkalinization of the interior compartments of the proteoliposomes was confirmed by an oxaloacetate-dependent accumulation of  $[^{14}C]$ acetate in this reservoir [34]. This assay is based on the fact that acetic acid moves freely across the membrane from the acidic into the alkaline compartment, where it becomes trapped by the dissociation to acetate which is membrane-impermeable. If the proton required for the decarboxylation of oxaloacetate stems from the interior reservoir of the proteoliposomes, more than one  $Na^+$  has to be pumped into this compartment to account for the electrogenicity of the pump [3]. In the initial phase of the reaction the  $Na^+$  to oxaloacetate stoichiometry is in fact close to two [40]. Later, when a membrane potential and/or a  $Na^+$  concentration gradient have developed the ratio drops, but the mechanistic details of this phenomenon are not well understood [40]. Evidence is available for two different  $Na^+$  binding sites on the decarboxylase operating together in the catalytic mechanism. The rate of oxaloacetate decarboxylation depends on the  $Na^+$  concentration, but does not follow a Michaelis–Menten relationship. Instead, the kinetic data could be well fitted by the Hill equation, yielding a Hill coefficient of 1.8 [35]. Hence, two different  $Na^+$  binding sites are present in the oxaloacetate decarboxylase which have to be occupied simultaneously in order to achieve the maximal activity of the enzyme. Half-maximal activation of the decarboxylase is obtained at about 0.7 mM  $Na^+$  [41]. Therefore, before the enzyme decarboxylates oxaloacetate, both sites must have  $Na^+$  binding affinities of at least 0.7 mM. Evidence is also available, however, that the enzyme contains low affinity  $Na^+$  binding sites ( $K_D \approx 20$  mM). Occupation of these sites with  $Na^+$  induces a conformational change in the  $\beta$  subunit which stabilizes the complex with the other two subunits under certain conditions and protects the  $\beta$  subunit from tryptic hydrolysis or from the denaturation by organic solvents [30,42].

In a  $Na^+$  pump like oxaloacetate decarboxylase  $Na^+$  binding sites with high and low affinity are postulated to exist in different states of the catalytic cycle. A possible pump cycle in which these and oth-

er observations have been included is shown in Fig. 7. In the first step, the carboxybiotin is formed with simultaneous conversion of oxaloacetate to pyruvate. Upon binding of the carboxybiotin to the  $\beta$  subunit catalytic site (species  $E^=(H^+) \sim CO_2^-$ ) the  $Na^+$  binding sites are exposed to the cytoplasm and are of high affinity. Binding of the two  $Na^+$  ions to these sites liberates a proton from S382 which is subsequently consumed in the decarboxylation of the carboxybiotin. The decarboxylation reaction is coupled to a conformational change of the protein by which the  $Na^+$ -occupied sites become exposed to the periplasm, and simultaneously, the  $Na^+$  binding affinities of these sites are reduced (species  $E^=(2Na^+_{out})$ ). Hence, the  $Na^+$  ions dissociate easily into the periplasmic reservoir, while a proton enters the channel from this side to restore the hydroxyl group of S382. To close the cycle, the unloaded form of the enzyme  $E^=(H^+)$  can undergo a conformational change to expose the  $Na^+$  binding sites again toward the cytoplasmic surface. This model is in accord with the finding of high affinity  $Na^+$  binding sites promoting the decarboxylation of the  $E^=(H^+) \sim CO_2^-$  species

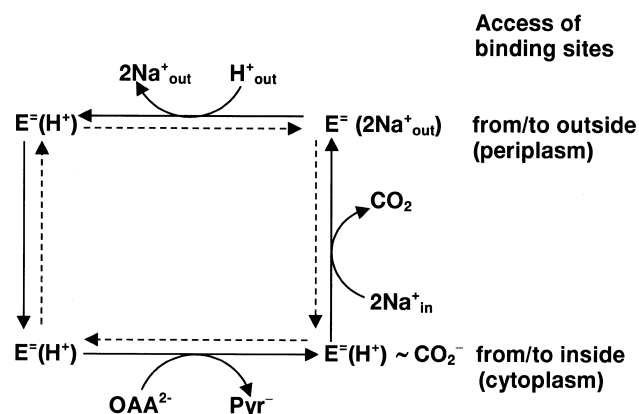


Fig. 7. Hypothetical pump cycle of the oxaloacetate decarboxylase  $Na^+$  pump.  $E^=(H^+)$  symbolizes enzyme with  $\beta$ -D203 deprotonated and  $\beta$ -S382 protonated and  $E^=$  symbolizes enzyme with  $\beta$ -D203 and  $\beta$ -S382 deprotonated.  $E^=(H^+) \sim CO_2^-$  is the carboxybiotin enzyme with  $\beta$ -S382 protonated. Bound  $Na^+$  ions are indicated in parentheses.  $OAA^{2-}$ , oxaloacetate;  $Pyr^-$ , pyruvate. The enzyme specimens shown at the top of the figure have their  $Na^+$  binding sites exposed toward the periplasm, and those shown at the bottom of the figure have their  $Na^+$  binding sites exposed toward the cytoplasm. The whole cycle is reversible, but for simplicity, substrate addition and product release reactions are only shown in the forward direction. For details see text.

[41] and of low affinity  $\text{Na}^+$  binding sites in the free enzyme [30,42]. Occupation of the low affinity sites converts the free enzyme into the  $\text{E}=(2\text{Na}_{\text{out}}^+)$  conformation which is resistant to tryptic hydrolysis or to denaturation by organic solvents. The reaction scheme is also in accord with the inhibition of oxaloacetate decarboxylation at elevated  $\text{Na}^+$  concentrations, which is especially pronounced at high pH [34]. These conditions are unfavorable for the  $\text{H}^+$ -dependent release of the two  $\text{Na}^+$  ions bound from the  $\text{E}=(2\text{Na}_{\text{out}}^+)$  specimen and this reaction therefore most likely becomes rate-limiting for the entire turnover.

The reaction scheme shown in Fig. 7 is also able to explain the reversibility of the pump [43]. At a high  $\text{Na}^+$  concentration on the outside and a low  $\text{Na}^+$  concentration on the inside the enzyme would convert from  $\text{E}=(\text{H}^+)$  via  $\text{E}=(2\text{Na}_{\text{out}}^+)$  to  $\text{E}=(\text{H}^+) \sim \text{CO}_2^-$ , where the downhill movement of two  $\text{Na}^+$  ions drives the carboxylation of biotin. The carboxyl group of carboxybiotin will subsequently be transferred to pyruvate to yield oxaloacetate. Another intriguing observation is the catalysis of a  $\text{Na}_{\text{in}}^+ / {}^{22}\text{Na}_{\text{out}}^+$  exchange in the absence of oxaloacetate or pyruvate. This exchange was strictly dependent on the presence of bicarbonate, it was completely inhibited by avidin and it was not catalyzed if the biotin-containing  $\alpha$  subunit was dissociated from the  $\beta$ - $\gamma$  complex [40]. These results indicate a strict coupling of the  $\text{Na}_{\text{in}}^+ / {}^{22}\text{Na}_{\text{out}}^+$  exchange with the carboxylation and decarboxylation of carboxybiotin. This is described by the conversion  $\text{E}=(2\text{Na}_{\text{out}}^+) + \text{CO}_2 \rightleftharpoons \text{E}=(\text{H}^+) \sim \text{CO}_2^- + 2\text{Na}_{\text{in}}^+$ .

## 8. Molecular model for energy coupling

Finally, the results from site-specific mutagenesis and from the biochemical characterizations of oxaloacetate decarboxylase have been combined in a working model for the energy coupling mechanism which is shown in Fig. 8 [35,39]. In this model, we envisage two different  $\text{Na}^+$  binding sites on the  $\beta$  subunit, one involving D203 and the other involving S382. Region IIIa, helix IV and helix VIII are proposed to align the channel for  $\text{Na}^+$  or for  $\text{H}^+$  moving in opposite orientation across the membrane. We further assume two different conformations of the

protein, one with the  $\text{Na}^+$  binding sites accessible from the cytoplasm and the other with the  $\text{Na}^+$  binding sites accessible from the periplasm. The catalytic cycle starts with the carboxylation of the biotin prosthetic group in the carboxyltransferase reaction on the  $\alpha$  subunit with oxaloacetate as carboxyl donor. In Fig. 8A the carboxybiotin residue has switched to the decarboxylase catalytic site on the  $\beta$  subunit. This binding may be facilitated by R389 which is close to the cytoplasmic surface within transmembrane helix VIII and may stabilize conformation 1 in which the two  $\text{Na}^+$  binding sites are accessible from the cytoplasm and have a high affinity for the alkali ion. After the first  $\text{Na}^+$  has bound to Asp203, the second  $\text{Na}^+$  approaches S382 (Fig. 8B) which is part of a proton-conducting network including Y229, R389,  $\text{H}_2\text{O}$  and carboxybiotin. R389 and carboxybiotin may have similar functions as the catalytic histidine and aspartate residues in serine proteases, i.e. to reduce the  $\text{pK}$  of S382. It is conceivable, therefore, that  $\text{Na}^+$  approaching S382 through the cytoplasmic channel can displace the proton from the hydroxyl side chain of S382, especially as the newly formed ion pair within the hydrophobic environment of the membrane would be thermodynamically more favorable than the presence of a  $\text{Na}^+$  ion with an unbalanced positive charge. This displacement might induce the rearrangement of hydrogen bonding within the network to ultimately deliver a proton to carboxybiotin to catalyze the immediate decarboxylation of this acid-labile compound. The reaction is proposed to initiate a change to conformation 2 by which the cytoplasmic channel closes and a periplasmic channel opens (Fig. 8B  $\rightarrow$  C). Once open, the two  $\text{Na}^+$  ions bound to the D203 and S382 including sites could be released through this channel into the periplasmic compartment. To displace the  $\text{Na}^+$  from S382, a periplasmic proton penetrating through the channel must restore the hydroxyl group of S382, because an uncompensated negative charge would not be tolerated near the center of the membrane for electrostatic reasons. For the proton to reach this deeply embedded membrane position, it could first bind to D203 near the periplasmic surface thereby releasing the first  $\text{Na}^+$  ion, and could be subsequently transmitted to S382 with the release of the second  $\text{Na}^+$  ion. An obligatory requirement of D203 and S382 in the proton translocation pathway is

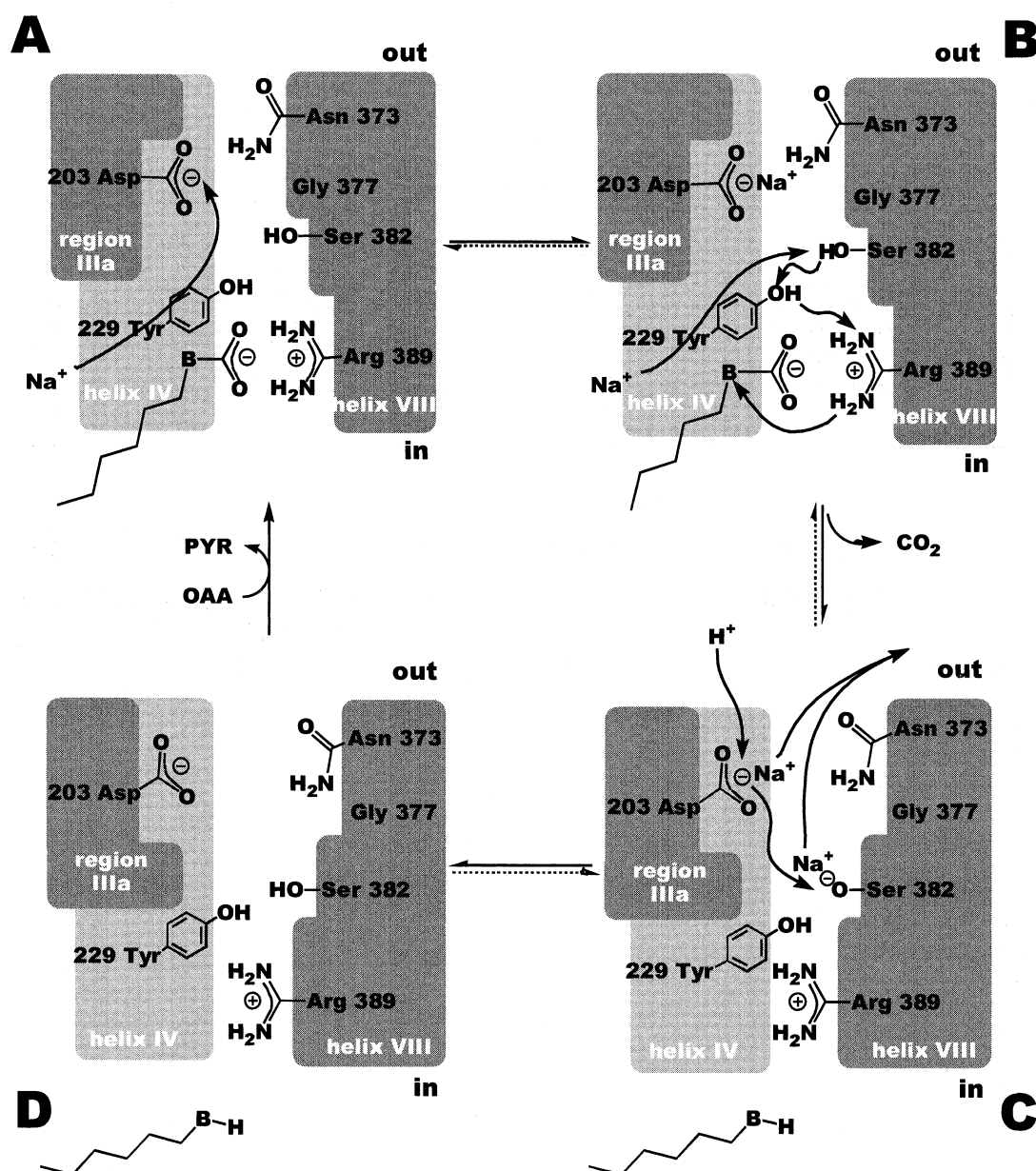


Fig. 8. Model for coupling Na<sup>+</sup> and H<sup>+</sup> movements across the membrane to the decarboxylation of carboxybiotin. The model shows the appropriate location of important residues of helix IV, helix VIII and of region IIIa of the β subunit. Also shown is the participation of these residues in the vectorial and chemical events of the Na<sup>+</sup> pump. Panel A shows the empty binding site region with enzyme-bound carboxybiotin (B-COO<sup>-</sup>), exposing the Na<sup>+</sup> binding sites toward the cytoplasm. Panel B shows the situation where the first Na<sup>+</sup> binding site at the D203-N373 pair has been occupied and the second Na<sup>+</sup> enters the S382 site with simultaneous release of the proton from the hydroxyl side chain. This displacement may lead to the rearrangement of hydrogen bonding in the network involving S382, Y229, R389 and carboxybiotin with the result that a proton is delivered to the carboxybiotin. This catalyzes the immediate decarboxylation of this acid-labile compound, involving a conformation change (B → C) which exposes the Na<sup>+</sup> binding sites toward the periplasm. The Na<sup>+</sup> ions are subsequently released into this reservoir, while a proton enters the periplasmic channel and restores the hydroxyl group of S382. In panel D, the Na<sup>+</sup> binding sites are empty and exposed toward the periplasm and the biotin prosthetic group is not modified (B-H). Upon carboxylation of the biotin, the protein switches back into the conformation where the Na<sup>+</sup> binding sites are exposed toward the cytoplasm (D → A).

compatible with the observation that the decarboxylase activity is completely abolished if either of these residues is mutated [34,35]. After these events, carboxybiotin formed by OadA by carboxyltransfer with oxaloacetate binds to OadB (Fig. 8D→A). This stabilizes conformation 1, and a new reaction cycle begins.

Two  $\text{Na}^+$  ions have been translocated in this cycle from the cytoplasmic into the periplasmic compartment and a periplasmic proton has been consumed in the decarboxylation of carboxybiotin. Hence, the proposed mechanism is in accord with the observed  $\text{Na}^+$  to oxaloacetate stoichiometry of two [40] and it is also in accord with the notion that a proton moves in the opposite direction of  $\text{Na}^+$  transport during the operation of the pump [34]. The model further explains the direct coupling of the chemical and the vectorial events of the pump including the observation that carboxylation and decarboxylation of the biotin prosthetic group are essential for  $\text{Na}^+$  translocation across the membrane [34]. Also in accord with the model is the strict dependence of oxaloacetate decarboxylation from  $\text{Na}^+$  ions [41] because the proton of S382 that is required for the decarboxylation can only be displaced by an approaching  $\text{Na}^+$  ion. Inhibition of oxaloacetate decarboxylation by high  $\text{Na}^+$  concentrations and high pH can also be explained by the model [34]. Under these conditions, it will be difficult to displace  $\text{Na}^+$  from the low affinity site(s) and progress of the reaction cycle will be retarded.

The mechanism is further supported by the complete knock-out of the carboxybiotin decarboxylase activity in mutants of D203, S382, and Y229, which suggests that these residues could be involved in the proton translocation pathway that is essential for the catalysis. Aspartate is the only amino acid tolerated at position 203 [34]. This is to be expected if D203 contributes ligands for  $\text{Na}^+$  binding within a coordination sphere with a well defined geometry. A similar situation has previously been recognized for the  $\text{Na}^+$  binding residues of subunit c of the ATPase from *P. modestum* [44]. S382 may be replaced by D but not by N, E, or Q. Hence, the side chain of amino acid 382 must carry a group that can switch between protonated and deprotonated states. Furthermore, the length of the side chain appears to be crucial, which again would be compatible with a function of S382

in  $\text{Na}^+$  liganding. Y229 cannot be replaced by F, which is difficult to explain by a purely structural role of this residue and could indicate an involvement in the proton relay system. The small activity seen upon replacement of Y229 by A would be in accord with this supposition because the small alanine side chain but not phenylalanine could allow a water molecule to enter this area in order to replace Y229 in the proton conduction network [39]. G377 is another critical residue of the  $\beta$  subunit [35] but as it lacks a side chain with a functional group, it probably has a structural role either to allow  $\text{Na}^+$  to pass at a narrow portion of the channel or to make close contact with another helix. N373 could act as a ligand for the D203 including  $\text{Na}^+$  binding site, since both residues are located near the periplasmic surface and since the N373L or N373D mutations showed only traces of residual oxaloacetate decarboxylase activity. Further in accord with this supposition is a dramatic increase of the  $\text{Na}^+$  concentration required for half-maximal activation of oxaloacetate decarboxylase from 0.7 mM (wild-type) to 10 mM in the N373D mutant (unpublished results). Perhaps, the enzyme could operate at low rates even without the efficient  $\text{Na}^+$  binding site at the D203/N373 pair, because D203 could still act as a proton carrier in the periplasmic channel. The decarboxylase activity was also markedly reduced but not abolished by mutating R389 to the neutral amino acids A or L, and even the R389D mutant retained some activity [35]. Hence, R389 is not an absolutely essential residue for function. However, its side chain may facilitate conduction of the proton from S382 through the network to carboxybiotin, thus enhancing its decarboxylation rate. A hint for this function is a drastic increase of the pH optimum in the R389A and R389L mutants.

In summary, we propose a molecular model for the coupling of the chemical reaction and the vectorial ion movements across the membrane by the oxaloacetate decarboxylase  $\text{Na}^+$  pump. The central feature of this mechanism is using membrane-buried amino acid residues (S382; the D203–N373 pair) as binding sites for the oppositely oriented movements of  $\text{Na}^+$  and  $\text{H}^+$ . The two sites take up  $\text{Na}^+$  ions from the cytoplasm and deliver them to the periplasm. Simultaneously, a proton is translocated across the membrane, following the opposite route

toward carboxybiotin, where it is consumed in catalyzing the decarboxylation of this acid-labile compound. This model very elegantly describes a direct coupling mechanism, where the  $\text{Na}^+$  movement triggers the oppositely oriented translocation of protons across the membrane into the catalytic site where they are consumed in the chemical event of the catalysis.

## References

- [1] P. Dimroth, *Biochim. Biophys. Acta* 1318 (1997) 11–51.
- [2] P. Dimroth, B. Schink, *Arch. Microbiol.* 170 (1998) 69–77.
- [3] P. Dimroth, *Eur. J. Biochem.* 121 (1982) 443–449.
- [4] W. Hilpert, P. Dimroth, *Eur. J. Biochem.* 132 (1983) 579–587.
- [5] W. Buckel, R. Semmler, *Eur. J. Biochem.* 136 (1983) 427–434.
- [6] H. Hilbi, I. Dehning, B. Schink, P. Dimroth, *Eur. J. Biochem.* 207 (1992) 117–123.
- [7] M. Hayashi, T. Unemoto, *Biochim. Biophys. Acta* 767 (1984) 470–478.
- [8] X.D. Pfenniger-Li, S.P.J. Albracht, R.M. van Belzen, P. Dimroth, *Biochemistry* 35 (1996) 6233–6242.
- [9] W. Krebs, J. Steuber, A.C. Gemperli, P. Dimroth, *Mol. Microbiol.* 33 (1999) 590–598.
- [10] J. Steuber, C. Schmid, M. Rufibach, P. Dimroth, *Mol. Microbiol.* 35 (2000) 428–434.
- [11] B. Becker, V. Müller, G. Gottschalk, *J. Bacteriol.* 174 (1992) 7656–7660.
- [12] P. Gärtner, D.S. Weiss, U. Harms, R.K. Thauer, *Eur. J. Biochem.* 226 (1994) 465–472.
- [13] K. Takase, S. Kakinuma, K. Yamato, K. Konishi, K. Igarashi, Y. Kakinuma, *J. Biol. Chem.* 269 (1994) 11037–11044.
- [14] E. Padan, S. Schuldiner, *J. Bioenerg. Biomembr.* 25 (1993) 647–669.
- [15] K.M. Pos, P. Dimroth, *Biochemistry* 35 (1996) 1018–1026.
- [16] S. Kojima, K. Yamamoto, I. Kawagishi, M. Homma, *J. Bacteriol.* 181 (1999) 1927–1930.
- [17] W. Laubinger, P. Dimroth, *Biochemistry* 27 (1988) 7531–7537.
- [18] W. Hilpert, B. Schink, P. Dimroth, *EMBO J.* 3 (1984) 1665–1670.
- [19] P. Dimroth, G. Kaim, U. Matthey, *J. Exp. Biol.* 203 (2000) 51–59.
- [20] E. Schwarz, D. Oesterheld, D. Reinke, K. Beyreuther, P. Dimroth, *J. Biol. Chem.* 263 (1988) 9640–9645.
- [21] G. Woehlke, E. Laußemair, E. Schwarz, D. Oesterheld, H. Reinke, K. Beyreuther, P. Dimroth, *J. Biol. Chem.* 267 (1992) 22798–22803.
- [22] J. Huder, P. Dimroth, *J. Biol. Chem.* 268 (1993) 24564–24571.
- [23] A. Braune, K. Bendrat, S. Rospert, W. Buckel, *Mol. Microbiol.* 31 (1999) 473–487.
- [24] M. Berg, H. Hilbi, P. Dimroth, *Eur. J. Biochem.* 245 (1997) 103–115.
- [25] P. Dimroth, H. Hilbi, *Mol. Microbiol.* 25 (1997) 3–10.
- [26] J. Steuber, W. Krebs, M. Bott, P. Dimroth, *J. Bacteriol.* 181 (1999) 241–245.
- [27] M. Bott, P. Dimroth, *Mol. Microbiol.* 14 (1994) 347–356.
- [28] M. Bott, M. Meyer, P. Dimroth, *Mol. Microbiol.* 18 (1995) 533–546.
- [29] K. Schneider, P. Dimroth, M. Bott, *Biochemistry* 39 (2000) 9438–9450.
- [30] P. Dimroth, A. Thomer, *Eur. J. Biochem.* 137 (1983) 107–112.
- [31] P. Dimroth, A. Thomer, *Eur. J. Biochem.* 175 (1988) 175–180.
- [32] P. Dimroth, A. Thomer, *FEBS Lett.* 300 (1992) 67–70.
- [33] M. Di Berardino, P. Dimroth, *Eur. J. Biochem.* 231 (1995) 790–801.
- [34] M. Di Berardino, P. Dimroth, *EMBO J.* 15 (1996) 1842–1849.
- [35] P. Jockel, M. Schmid, J. Steuber, P. Dimroth, *Biochemistry* 39 (2000) 2307–2315.
- [36] P. Dimroth, *Methods Enzymol.* 125 (1986) 530–540.
- [37] P. Jockel, M. Di Berardino, P. Dimroth, *Biochemistry* 38 (1999) 13461–13472.
- [38] E. Pinner, Y. Kolter, E. Padan, S. Schuldiner, *J. Biol. Chem.* 268 (1993) 1729–1734.
- [39] P. Jockel, M. Schmid, T. Choinowski, P. Dimroth, *Biochemistry* 39 (2000) 4320–4326.
- [40] P. Dimroth, A. Thomer, *Biochemistry* 31 (1993) 1734–1739.
- [41] P. Dimroth, A. Thomer, *Eur. J. Biochem.* 156 (1986) 157–162.
- [42] W. Buckel, H. Liedtke, *Eur. J. Biochem.* 156 (1986) 251–257.
- [43] P. Dimroth, W. Hilpert, *Biochemistry* 23 (1984) 5360–5366.
- [44] G. Kaim, F. Wehrle, P. Dimroth, *Biochemistry* 36 (1997) 9185–9194.